Radio Frequency Magnetic Field Limits of Nb and Nb_3Sn

S. Posen,* N. Valles,† and M. Liepe
Cornell Laboratory for Accelerator-Based Sciences and Education, Ithaca, New York 14853, USA
(Received 5 March 2015; published 21 July 2015)

Superconducting radio frequency (srf) cavities, essential components of many large particle accelerators, rely on the metastable flux-free state of superconducting materials. In this Letter, we present results of experiments measuring the magnetic field limits of two srf materials, Nb and Nb_3Sn. Resonators made using these materials were probed using both high power rf pulses and dc magnetic fields. Nb, which is the current standard material for srf cavities in applications, was found to be limited by the superheating field H_{sh} when prepared using methods to avoid excessive rf dissipation at high fields. Nb_3Sn, which is a promising alternative material that is still in the early stages of development for srf purposes, was found to be limited between the onset field of metastability H_{c1} and H_{sh}. Analysis of the results shows that the limitation is consistent with nucleation of flux penetration at defects in the rf layer.

DOI: 10.1103/PhysRevLett.115.047001 PACS numbers: 74.70.Ad, 74.25.nn, 74.25.Op

Superconducting radio frequency (srf) cavities are devices that transfer energy to charged particle beams in applications such as light sources [1,2], neutron sources [3,4], and colliders [5,6]. When rf power is applied to a cavity close to its resonant frequency, it builds up large electromagnetic fields. The electric field that is generated accelerates the beam as it passes through the cavity, but a magnetic field is also produced, which interacts with the superconductor on the cavity surface. For sufficiently large magnetic fields, the superconductor will quench, i.e., be driven normal conducting.

To remain superconducting, srf materials generally operate in the Meissner state, in which flux is completely expelled from the material. For sufficiently high external fields, type II superconductors will leave the Meissner state and enter the vortex state, in which a lattice of magnetic flux lines permeates the material, threading through normal conducting vortex cores. However, as the direction of the magnetic field reverses, these normal cores would have to move in and out of the material, which is a highly dissipative process [7]. At rf frequencies, the dissipation from bulk flux penetration is strong enough to bring the superconductor above its critical temperature, T_c.

It is important to understand what magnitude of external magnetic field will cause flux penetration, because this limits the usefulness of srf materials in applications. Consider a flux-free superconductor in an external field that is slowly increased. The field at which the first fluxoid penetrates is determined by a competition between (i) the external fields, which generate a force pushing the fluxoid into the material and (ii) the fields generated by vortex currents, the effect of which can be interpreted as an image vortex pulling the fluxoid out of the material [8]. The field at which it becomes energetically favorable for flux to be inside the bulk of a type II superconductor is the lower critical field H_{c1}, though flux penetration will not necessarily occur at this field. An energy barrier at the surface of the material allows it to remain in a metastable flux-free state up to, at most, the superheating field H_{sh} [9].

Two materials that are relevant for srf applications are Nb and Nb_3Sn. Nb is the current standard material—srf cavities are commonly formed and welded from purified Nb sheets, then given treatments that have been developed over decades of research to maximize accelerating gradients and minimize resistive losses. Nb_3Sn has had much less development than Nb, but it has been demonstrated that cavities made from this material can achieve extremely high quality factors (i.e., very small surface resistance) even at relatively high temperatures, and its predicted H_{sh} is approximately twice that of Nb [10]. On the other hand, it also has a comparatively small coherence length ξ (see examples of material properties in Table I), which sets the length scale for defects that can interrupt the surface energy barrier. As a result, even relatively small surface defects may act as nucleation sites for flux penetration. Understanding the relationship between ξ and the maximum surface fields these materials can support in the Meissner state has been attempted in previous experiments with limited success. It remains an important goal in order to evaluate the potential for Nb_3Sn to replace Nb in future srf applications.

In this Letter, we review these previous experiments and present new results probing the magnetic field limits of the metastable Meissner states of state-of-the-art Nb and Nb_3Sn, prepared as they would be for srf applications. The two types of probes used are short, high power rf pulses and

TABLE I. Comparison of parameters obtained during cw tests. Except where noted, parameters are given at $T = 0$. For details of cw testing and material parameter extraction, see Refs. [11,12].

Preparation No. Treatment	1 EP	2 EP + 120 °C bake	3 BCP + Nb_3Sn coating	4 BCP + Nb_3Sn coating
T_c [K]	9.2 ± 0.2	8.8 ± 0.2	18.0 ± 0.1	18.0 ± 0.1
λ [nm]	45 ± 3	80 ± 18	161 ± 25	198 ± 50
ξ [nm]	25 ± 2	14 ± 3	3.0 ± 0.4	2.4 ± 0.6
$\mu_0 H_{c1}$ [mT]	121 ± 7	59 ± 20	29 ± 2	21 ± 2
$\mu_0 H_{sh}$ [mT]	241 ± 24	198 ± 63	399 ± 81	390 ± 134
cw limitation at 2 K	HFQS	Quench	Quench	Quench
$\mu_0 H_{pk}$ at limitation [mT]	104 ± 10	182 ± 18	55 ± 6	62 ± 6

external dc magnetic fields. We compare the maximum fields measured to H_{c1} and H_{sh} of the materials, and discuss possible reasons that H_{sh} is not reached in some cases. We conclude with an outlook for increasing maximum surface fields in the future.

Two single cell 1.3 GHz bulk niobium cavities were used in this research. In what shall be called preparation 1, one of the cavities was only electropolished (EP) [13,14] before testing. In preparation 2, it was both EP and baked at 120 °C for 48 h, a process that diffuses oxygen from niobium's natural oxide into the surface layer where rf currents flow [15]. It has been established that the combination of electropolishing and 120 °C bake of Nb cavities prevents high field Q slope (HFQS), a sharp increase in surface dissipation observed at an onset field on the order of 100–120 mT [16,17] (many theories have been postulated for the cause of this degradation, e.g., Refs. [18–23]—see also the review in Ref. [24]). In preparations 3 and 4, the second cavity was given a buffered chemical polish (BCP) and coated with Nb_3Sn (layer ~10 penetration depths thick) via the vapor diffusion process [25–28]. The Nb_3Sn preparation procedure carried out at Cornell was recently shown to avoid a strong dissipation mechanism observed in previous experiments (see Refs. [29–31] for additional details of Cornell's Nb_3Sn fabrication process and results).

For each preparation, the cavity was tested in the continuous wave (cw) mode. Material parameters were extracted from measurements of quality factor and frequency as a function of temperature, and they were used to calculate the critical fields of the material in the rf surface. These material parameters and critical fields are shown in Table I, along with the limitation encountered in cw testing and the peak surface magnetic field H_{pk} at the limitation. For niobium, which is only weakly type II, H_{c1} was calculated by interpolation from the numerical calculations in Refs. [32,33]. For the strongly type II Nb_3Sn, H_{c1} was calculated using equations in Ref. [32]. H_{sh} was calculated using equations in Ref. [34].

For preparations 1–3, measurements were performed in pulsed mode. rf forward power pulses with power on the order of 1 MW and duration on the order of 100 μs were generated by a klystron to rapidly increase fields inside the SRF cavities. Using the procedure described in Ref. [35], the quench field H_{quench} was measured as a function of temperature. Cavity temperature was recorded with Cernox sensors in good thermal contact with its surface. The results are shown in Fig. 1. Also plotted in the figure are H_{c1} and H_{sh} for each preparation, using the zero temperature values from Table I and the expected trend with temperature T, approximately $1 - (T/T_c)^2$ [36].

In preparation 2, the niobium cavity received both electropolish and bake to prevent degradation from HFQS, and H_{quench} is very close to the ultimate limit H_{sh}. H_{sh}, H_{c1}, and T_c are all somewhat smaller than the values for clean niobium, due to the addition of impurities to the rf layer from the baking process. Preparation 1, which omits the bake, also has quench field close to H_{sh} near T_c, but at lower temperatures, H_{sh} is larger than could be reached using the high power rf pulses. This is due to the onset of the very strong HFQS in this cavity, which causes significant thermal heating and prevents it from reaching higher fields, even with the 1 MW pulses used [39]. These observations are consistent with pulsed experiments carried out at Cornell on an unbaked cavity by Hays *et al.* [35].

The Nb_3Sn cavity shows good agreement near T_c between the pulsed quench field and H_{sh}. At lower temperatures, the quench field is significantly smaller than H_{sh}, reaching the highest values of just over 100 mT when $T \ll T_c$. Through the entire temperature range, H_{quench} is considerably higher than H_{c1}, showing that the onset of metastability does not limit the material. Similar measurements were performed by Campisi [40] and Hays *et al.* [35], also plotted. Both experiments show a trend towards flat $H_{quench}(T)$ at low temperatures. In Nb, flat $H_{quench}(T)$ is caused by HFQS limitation. In Nb_3Sn, this behavior may also be caused by a thermal heating limitation, for example, from defects on the surface that nucleate local flux penetration.

Surface defects have been studied as a possible cause for the trend in Hays's data sets, which agree well with an approximately $1 - (T/T_c)^4$ trend, rather than a quadratic dependence [41]. This is consistent with some theoretical models of vortex penetration [42], which deal not with fundamental limitations on ideal surfaces, but rather

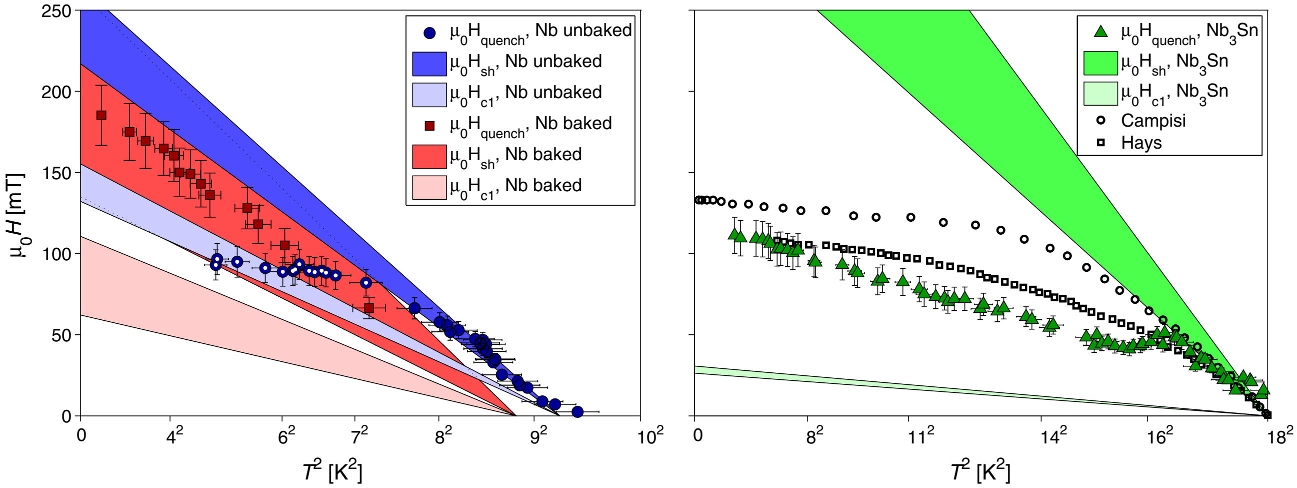

FIG. 1 (color online). Measured quench field of Nb (left) and Nb_3Sn (right) superconducting cavities under high power rf pulses as a function of temperature. For niobium, the cavity was tested both with bake to prevent limitation from HFQS and without it; the measurements that appear to be affected by HFQS are marked with white points at their centers. The dark and light shaded bands show the approximate temperature dependence of H_{sh} and H_{c1} extracted from CW measurements.

nucleation on surface imperfections [9] (for example, the heuristic vortex line nucleation model (VLNM) has shown some success in describing this as well as other experimental data [41,43]). In Fig. 2, goodness-of-fit statistics are shown for the results presented here, as well as those from Hays *et al.* and from Campisi, using $H_{\mathrm{quench}} = H_0[1 - (T/T_c)^n]$, where H_0 is a fitting parameter and $n = 2$ or 4. The new experimental results allow a comparison between a cavity prepared such that it consistently reached fields close to the ultimate superheating limit, and several cavities that quench at fields significantly below this. Only the baked niobium shows better agreement with the $n = 2$ function predicted for an ideal surface, indicating that the nonideal performances may be caused by imperfect surfaces.

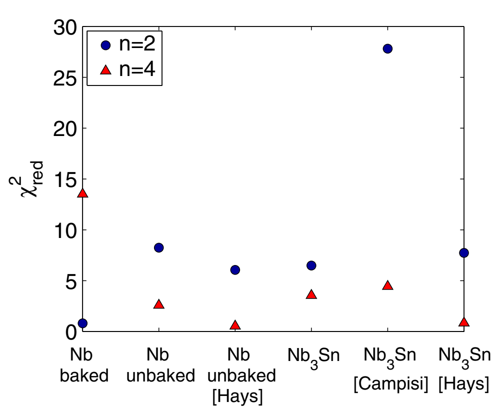

FIG. 2 (color online). Goodness of fit statistics to pulsed quench field data. The two models represent different types of surfaces: ideal ones ($n = 2$) and those with imperfections ($n = 4$). χ^2_{red} of 1 indicates good agreement between data and model within the estimated variance of 5 mT. $\chi^2_{\mathrm{red}} \gg 1$ indicates a poor fit.

To further study the limitation in the Nb_3Sn cavity, measurements were performed at 4.2 K with varying forward power P_f from the klystron, as shown in Fig. 3. If a fundamental field limit were being reached, the quench field should not depend on P_f. However, as P_f is increased, H_{quench} is observed to increase as well. This trend would be consistent with thermal heating limitations: with a higher forward power, a given field level in the cavity is reached faster, leaving less time for heating of the surface, and therefore a higher quench field is reached. A simple model for this thermal limitation was applied to the data, in which we assume that thermal diffusion is slow compared to the duration of the rf pulse. We then balance the rf energy deposited in the rf surface and the heat required to drive it normal conducting. The result is shown in the figure. Surface heating resulting from defects would also be consistent with the recent observation of low tin content

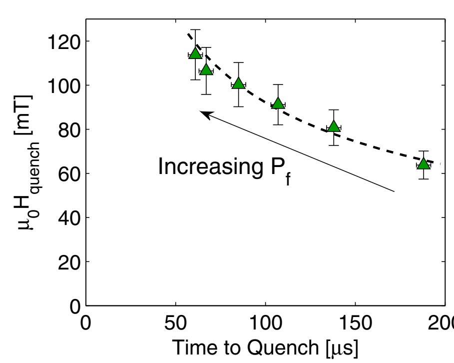

FIG. 3 (color online). Pulsed 4.2 K quench field in the Nb_3Sn cavity as a function of the time it takes to raise the field until quench occurs with uniform forward power. The time to quench was varied by changing P_f from the klystron. The dashed line shows a fit to the measurement using a simple thermal model.

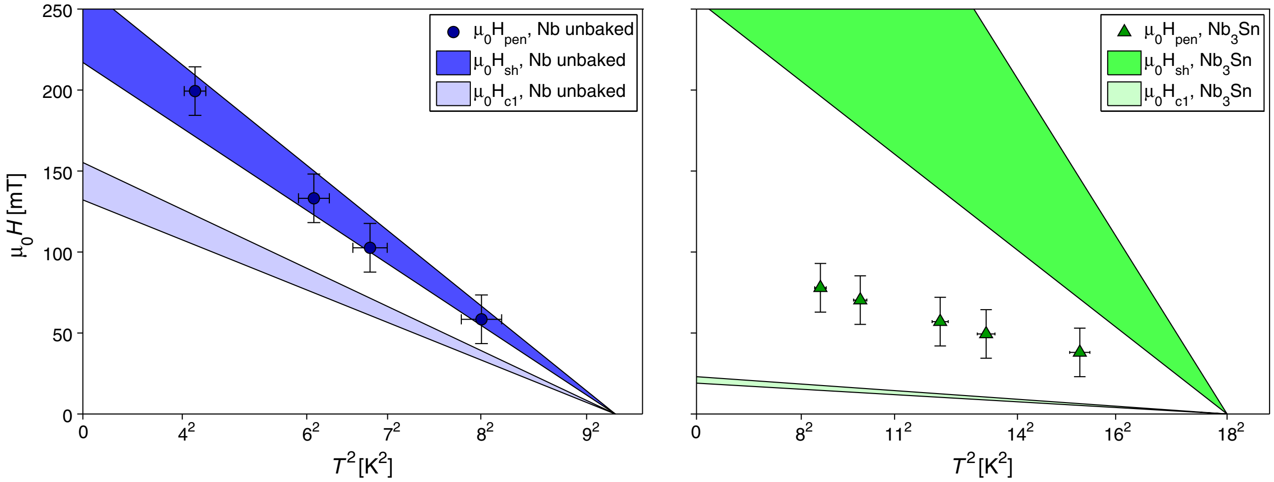

FIG. 4 (color online). Measured flux penetration field of Nb (left) and Nb_3Sn (right) superconducting cavities under an external dc magnetic field as a function of temperature. The dark and light shaded bands show the approximate temperature dependence of H_{sh} and H_{c1} extracted from cw measurements.

regions near the surface of a witness sample coated with the cavity [44].

dc magnetic field measurements were performed for preparations 1 and 4. In these experiments, a solenoid was fixed next to the cavity, with a magnetic field probe between them. A small amount of rf power was applied to the cavity, allowing its quality factor to be monitored as the dc current in the solenoid was increased. Penetration of the dc field into the rf layer would cause a sharp decrease in the quality factor. When this occurred, the magnetic field read by the probe would be recorded. A correction factor of 1.9 ± 0.2 was applied to determine the corresponding field at the rf surface, taking into account the effect of Meissner screening on the field distribution (details of the calculation can be found in Ref. [11]). In this way, the dc flux penetration field H_{pen} was determined as a function of temperature, as shown in Fig. 4.

The unbaked niobium of preparation 1 shows good agreement with $1 - (T/T_c)^2$ scaling of H_{sh}, reaching fields as high as ~200 mT at 4.2 K. Unlike the pulsed measurement—where HFQS causes strong dissipation at rf fields ~100 mT—the dc measurement probes the flux penetration field without rf-induced thermal effects being a concern. Preparation 2 could also be probed using this method, but the thin interior layer affected by the bake has a smaller H_{sh} than the clean niobium of the bulk, so one would expect to measure a similar dc penetration field to the unbaked cavity.

It is, however, illustrative to examine the Nb_3Sn cavity at $T > T_c$ of niobium, where only the Nb_3Sn is superconducting. The results again show a maximum flux-free field between H_{c1} and H_{sh}. In this measurement, thermal effects should not affect the result, but surface defects such as grain boundaries and off-stoichiometric regions can act as nucleation sites for flux penetration. In addition, there is a difference in the boundary conditions for the theoretical prediction compared to the experiment. In the experiment, the magnetic field is applied from outside the cavity, so that the relevant interface is the transition from the normal conducting niobium bulk to the superconducting Nb_3Sn. This boundary condition is not applied in the calculation, but rather that of a vacuum-to-superconductor interface (as it is for the internal fields of srf cavities). No prediction for the low temperature superheating field could be found in the literature when the more difficult boundary condition was applied involving a normal conducting metal.

In this Letter, we have presented new results and reviewed previous results exploring the rf magnetic field limits of superconducting Nb and Nb_3Sn using pulsed rf and dc probes. The results show that state of the art high field preparation techniques cause the pulsed quench field of Nb to closely follow H_{sh}. In Nb without the proper preparation, thermal effects due to the HFQS limit the quench field far below this. Pulsed measurements on a Nb_3Sn cavity also show a low temperature quench field below H_{sh}. One possible explanation that is consistent with both pulsed and dc measurements is flux penetration at defects in the Nb_3Sn surface. This was demonstrated by showing, in several experiments in which the field was limited significantly below H_{sh}, an approximate $1 - (T/T_c)^4$ temperature dependence, as predicted by theoretical models of vortex nucleation on surface imperfections [41,42]. Calculations based on extracted material parameters indicate that H_{c1} of Nb_3Sn is not a fundamentally limiting field. Future Nb_3Sn research will focus on optimizing parameters used in the coating process in order to reduce the presence of defects in the material, with a focus on low tin content regions that have been observed near the surface [44].

Work supported by NSF Career Grant No. PHY-0841213, NSF Grant No. PHY-1416318, DOE Grant No. ER41628, and the Alfred P. Sloan Foundation.

*Present address: Fermi National Accelerator Laboratory, Batavia, Illinois 60510, USA.
sep93@cornell.edu
†Present address: Raytheon Co., El Segundo, California, USA.

[1] J. N. Galayda, *Proceedings of the Fifth International Particle Accelerator Conference, Dresden, Germany* (2014).
[2] *Cornell Energy Recovery Linac Science Case and Project Definition Design Report*, Technical Report, edited by G. H. Hoffstaetter, S. M. Gruner, and M. Tigner, (Cornell University Laboratory for Accelerator-based Sciences and Education, 2013).
[3] T. E. Mason *et al.*, Physica (Amsterdam) **385B–386B**, 955 (2006).
[4] *European Spallation Source: Conceptual Design Report*, Technical Report, edited by S. Peggs (ESS, Lund, 2012).
[5] O. S. Brüning, P. Collier, P. Lebrun, S. Myers, R. Ostojic, J. Poole, and P. Proudlock, *CERN Geneva*, Technical Report (CERN, Geneva, 2004).
[6] T. Behnke, J. E. Brau, B. Foster, J. Fuster, M. Harrison, J. M. Paterson, M. Peskin, M. Stanitzki, N. Walker, and H. Yamamoto, *The International Linear Collider*, Technical Report (Technical Design Report, 2013).
[7] J. Bardeen and M. Stephen, Phys. Rev. **140**, A1197 (1965).
[8] C. Bean and J. Livingston, Phys. Rev. Lett. **12**, 14 (1964).
[9] J. Matricon and D. Saint-James, Phys. Lett. **24A**, 241 (1967).
[10] H. Padamsee, J. Knobloch, and T. Hays, *RF Superconductivity for Accelerators* (Wiley-VCH, New York, 2008), p. 521.
[11] N. R. Valles, Ph.D. thesis, Cornell University, 2014.
[12] S. Posen, Ph.D. thesis, Cornell University, 2015.
[13] H. Diepers, O. Schmidt, H. Martens, and F. Sun, Phys. Lett. **37A**, 139 (1971).
[14] K. Saito and Y. Kojima, *Proceedings of the Fourth Workshop on RF Superconductivity, Tsukuba, Japan* (1989).
[15] G. Ciovati, J. Appl. Phys. **96**, 1591 (2004).
[16] B. Visentin, TESLA Meet. DESY 98-05 (1998).
[17] P. Kneisel, *Proceedings of the Fourth Workshop on RF Superconductivity, Tsukuba, Japan* (1999), p. 328.
[18] A. Romanenko and H. Padamsee, Supercond. Sci. Technol. **23**, 045008 (2010).
[19] T. Proslier, J. F. Zasadzinski, L. Cooley, C. Antoine, J. Moore, J. Norem, M. Pellin, and K. E. Gray, Appl. Phys. Lett. **92**, 212505 (2008).
[20] G. Ciovati, Appl. Phys. Lett. **89**, 022507 (2006).
[21] J. Knobloch, R. Geng, M. Liepe, and H. Padamsee, *Proceedings of the Ninth Workshop on RF Superconductivity, Santa Fe, NM* (1999), p. 77, http://accelconf.web.cern.ch/AccelConf/SRF99/INDEX.htm.
[22] A. Gurevich, Physica (Amsterdam) **441C**, 38 (2006).
[23] W. Weingarten, Phys. Rev. ST Accel. Beams **14**, 101002 (2011).
[24] H. Padamsee, *RF Superconductivity: Volume II: Science, Technology and Applications* (Wiley-VCH, Weinheim, 2009).
[25] E. Saur and J. Wurm, Naturwissenschaften **49**, 127 (1962).
[26] G. Arnolds and D. Proch, IEEE Trans. Magn. **13**, 500 (1977).
[27] B. Hillenbrand, *Proceedings of the First Workshop on RF Superconductivity* (Karlsruhe, 1980).
[28] M. Peiniger, M. Hein, N. Klein, G. Müller, H. Piel, and P. Thuns, *Proceedings of the Third Workshop on RF Superconductivity* (Argonne National Laboratory, Lemont, 1988).
[29] S. Posen and M. Liepe, *Proceedings of the Fifteenth Conference on RF Superconductivity* (Chicago, 2011), pp. 886–889.
[30] S. Posen and M. Liepe, Phys. Rev. ST Accel. Beams **17**, 112001 (2014).
[31] S. Posen, M. Liepe, and D. L. Hall, Appl. Phys. Lett. **106**, 082601 (2015).
[32] M. Hein, *High-Temperature-Superconductor Thin Films at Microwave Frequencies* (Springer, New York, 1999).
[33] J. Harden and V. Arp, Cryogenics **3**, 105 (1963).
[34] M. K. Transtrum, G. Catelani, and J. P. Sethna, Phys. Rev. B **83**, 094505 (2011).
[35] T. Hays and H. Padamsee, *Proceedings of the Eighth on RF Superconductivity* (Padova, 1997), p. 789.
[36] This dependence is approximate. The temperature dependence of H_c is close to this [37], but other critical fields have additional dependence on the Ginzburg Landau parameter κ which will give an additional small correction (see, e.g., Ref. [38]).
[37] M. Tinkham, *Introduction to Superconductivity* (Dover, New York, 2004), p. 454.
[38] G. Catelani and J. P. Sethna, Phys. Rev. B **78**, 224509 (2008).
[39] This is supported by the dc measurements below showing flux penetration fields close to H_{sh}.
[40] I. Campisi, IEEE Trans. Magn. **21**, 134 (1985).
[41] K. Saito, *Proceedings of the Eleventh Workshop on RF Superconductivity* (Lübeck/Travemünder, 2003), p. MOO02.
[42] T. Yogi, G. J. Dick, and J. E. Mercereau, Phys. Rev. Lett. **39**, 826 (1977).
[43] T. Junginger, Ph.D. thesis, Ruperto-Carola University of Heidelberg, 2012.
[44] C. Becker, S. Posen, N. Groll, R. Cook, C. M. Schlepütz, D. L. Hall, M. Liepe, M. Pellin, J. Zasadzinski, and T. Proslier, Appl. Phys. Lett. **106**, 082602 (2015).